Pergamon

Journal of Structural Geology, Vol. 20, No. 9/10, pp. 1261 to 1272, 1998

0191-8141/98/$ - see front matter

PII: S0191-8141(98)00066-2

Stoped blocks in plutons: paleo-plumb bobs, viscometers, or chronometers?

S. R. PATERSON

Department of Earth Sciences, University of Southern California, Los Angeles, CA 90089-0740, U.S.A.
E-mail: paterson@usc.edu

and

R. B. MILLER

Department of Geology, San Jose State University, San Jose, CA 95192-0102, U.S.A.

(*Received* 1 *July* 1997; *accepted in revised form* 20 *April* 1998)

Abstract—Stoped blocks potentially provide information about paleohorizontal during emplacement of plutons, and about the timing of, and viscosities and kinematics during magmatic fabric formation. In the Mount Stuart batholith, Washington, we have examined magmatic fabrics patterns around stoped blocks in tonalite located near the pluton roof and completed 1:1 scale, three-dimensional mapping of fabric patterns around stoped blocks in diorite located ~1000 m below the roof. In both settings, no structural record of magma ascent, early emplacement, or settling of the blocks is preserved. Instead, fabric formation largely post-dates the settling and trapping of stoped blocks. Two-dimensional finite difference thermal modeling and calculations of sinking rates support short ($<2\times10^3$ years) residence times in the magma chamber for these blocks. Relatively symmetric foliation deflections around blocks indicate largely coaxial flattening during fabric formation and that magma viscosity must be lower than the viscosity of the weakest block (metapsammite) but high enough to trap the most dense block (dunite). Block settling calculations indicate that effective magma viscosities were from 10^{14} to 10^{15} Pa s and/or that yield strengths were large, which suggests that preserved fabrics formed in crystal-rich magmas near the tonalite and diorite solidi. Thus in the Mount Stuart batholith, stoped blocks fail to record information about paleohorizontal, but do indicate that the magmatic fabrics formed after chamber construction, during coaxial strain, and in crystal-rich magma near its solidus.

INTRODUCTION

Stoped blocks, although not volumetrically significant in most intrusions, occur in small numbers in many plutons and are particularly prevalent near pluton roofs (e.g. Buddington, 1959; Paterson *et al*., 1996). Besides providing information about emplacement mechanisms (e.g. Clarke *et al*., 1998), stoped blocks are potentially useful in several other ways. In this paper, we explore some of these uses in the hope that others will more closely examine stoped blocks in plutons elsewhere. As one example, we present results from our own study of stoped blocks in the Mount Stuart batholith, Washington.

With the advent of paleomagnetic studies, determining paleohorizontal during emplacement of plutons became an important issue (Beck *et al*., 1981; Haeussler and Paterson, 1993; Ague and Brandon, 1996). One means to potentially evaluate paleohorizontal is by the examination of stoped blocks. Stoped blocks that sink in a relatively static chamber will move vertically downwards and disturb any preexisting fabrics and/or layering (Fig. 1a). Even if magma is moving slowly, the sinking rate of medium-sized to large blocks will greatly exceed likely flow rates of magma residing in large chambers (e.g. Marsh, 1982). Cruden (1988) and Schmeling *et al*. (1988) provide excellent examples of the expected paths of objects sinking through Newtonian materials with pre-existing passive markers. Immediately below and on the sides of the object large strains rotate pre-existing fabrics towards the object margin, then laterally around the object. Large strains and thus fabric deflections occur out to several body radii (Fig. 1a). Constrictional, vertically oriented strains or zones of complex flow occur behind the sinking objects forming steeply plunging lineations or potentially randomizing fabrics if blocks sink rapidly. If such paths can be recognized in the field, then the line of symmetry through the path represents a vertical line of descent, or plumb line, at the time of sinking of the block (Fig. 1a). A statistical average of many such paleo-plumb lines measured in differently oriented planes could be obtained to average out any sideways motion caused by block tumbling, local flow of melts, or dispersion due to interaction of blocks.

The above discussion indicates that stoped blocks are also potentially useful time markers for determining when magmatic structures formed relative to chamber ascent and/or growth. Stoping represents one means by which a chamber can ascend or grow laterally. Any stoped block still preserved in the chamber

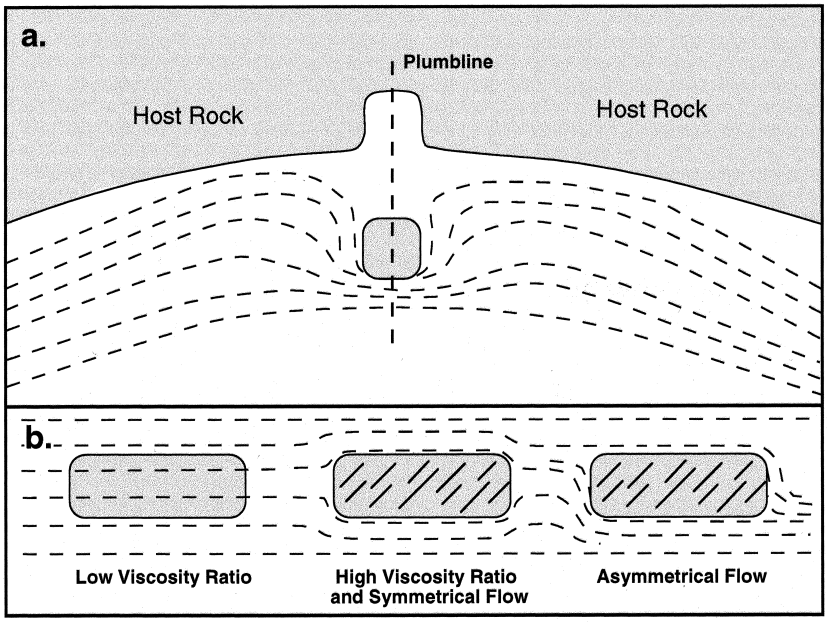

Fig. 1. (a) Cartoon showing pattern of fabric deflection (assuming original margin parallel fabric near a roof) around a sinking stoped block or 'paleo-plumb bob', and (b) patterns of fabric deflections around stoped blocks with different viscosity contrasts and/or coaxial or noncoaxial strain of magma. The first two blocks show coaxial shortening around blocks with low and high viscosity contrasts relative to surrounding magma, respectively: non-coaxial flow and high viscosity contrasts are shown for the last block.

and denser than the magma probably represents one of the last blocks to form. Thus, the time of sinking of the block reflects the last stages of chamber growth/ascent. This is particularly true near the roof of the pluton where it is sometimes possible to determine where a block originated. If the settling of such a stoped block disturbs magmatic fabrics, then fabric formation pre-dates final growth/ascent of the chamber (Fig. 1a). However, if fabrics wrap around the stoped block (Fig. 1b), then the fabrics formed during or after the block settled and became trapped at its preserved location, that is during or after final chamber growth.

Although methods of determining kinematics during magmatic fabric formation already exist (e.g. Nicolas, 1992), their application is commonly time consuming or fraught with uncertainty. Thus, additional methods of determining kinematics associated with magmatic fabrics would be useful. The symmetry of foliation patterns around stoped blocks is one such potential method (Fig. 1b), the application of which is identical to determining kinematics around resistant objects in metamorphic rocks.

Finally, stoped blocks may provide some information about the viscosity of melts. Because melt viscosities change by many orders of magnitude during ascent and crystallization, and because calculating viscosities from empirical equations or from experiments has proved difficult (e.g. Webb and Dingwell, 1990; Bergantz and Dawes, 1994; Lejeune and Richet, 1995), viscosities during ascent, emplacement, and fabric formation have remained controversial. Information about relative magma viscosities is available by comparing the degree of deflection of magmatic foliations near stoped blocks as has been done in strain analyses (e.g. Gay, 1968). The greater the deflection of magmatic fabrics around the stoped block, the greater the viscosity ratio between the two (Fig. 1b). Additional constraints on magma viscosity might be obtained by comparing foliation deflections around a number of stoped blocks with different viscosities and densities and calculating the magma viscosities/densities needed to trap these stoped blocks. The latter part of this procedure is essentially the same as that done to determine viscosity in experiments using spherical balls of known size and density (e.g. Dingwell *et al.*, 1993). Magma viscosities during fabric formation must then be less than (if fabrics are deflected around the block) or equal to (no deflection of fabrics) the viscosity of the stoped block, but large enough, or the magmas dense enough, to trap the blocks from sinking farther. Below we provide an example of these uses of stoped blocks.

EXAMPLE FROM MOUNT STUART BATHOLITH

The 93 Ma Mount Stuart batholith, located in the southern Cascades core, Washington, consists of two large bodies, a smaller southwestern elliptical body and larger northeastern body. The northeastern body, which contains the stoped blocks discussed in this paper, has a mushroom-shaped southeastern end, the stem of which extends northwest into a sheet-like central region and eventually into a hook-shaped north-

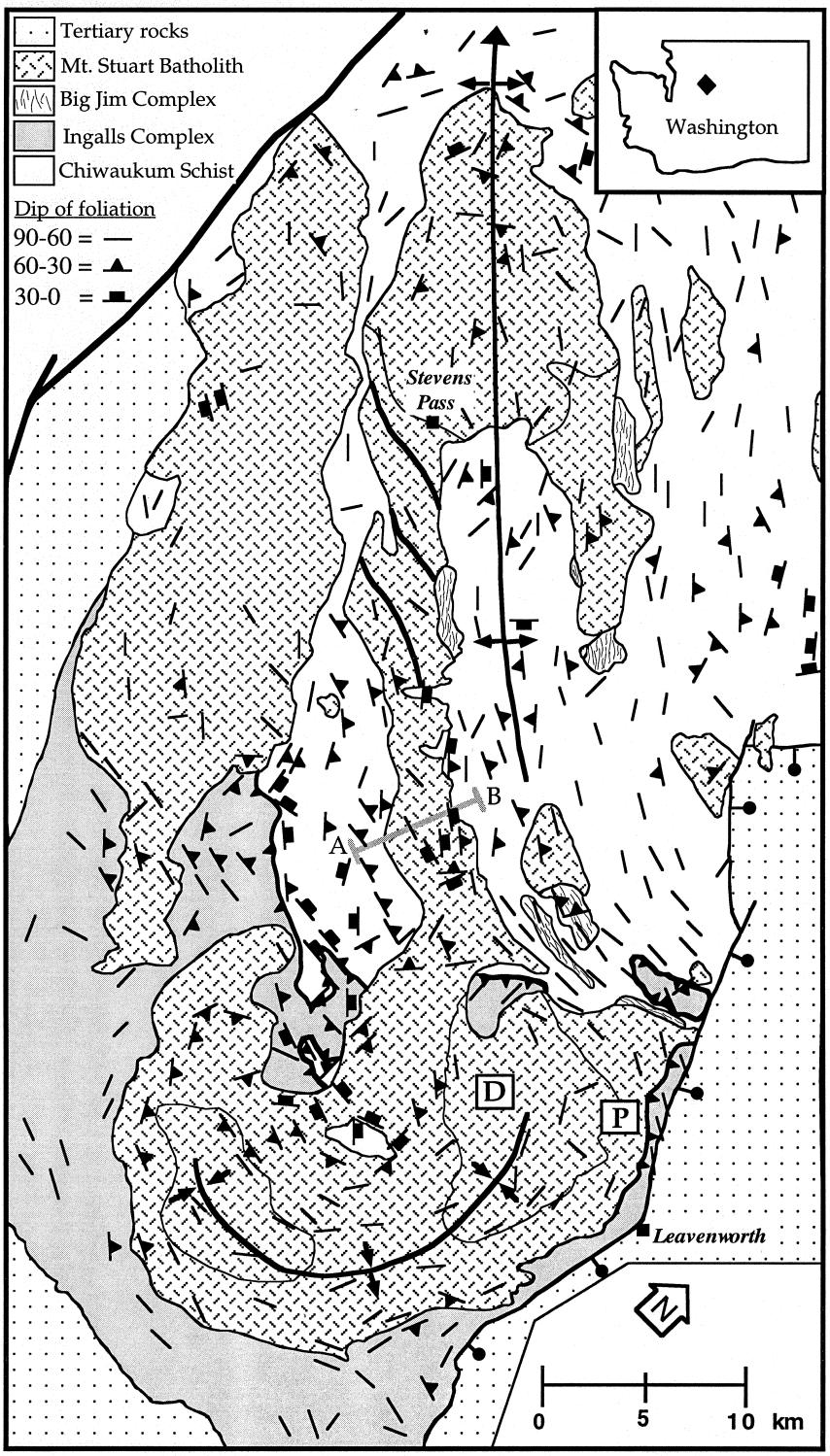

Fig. 2. Map of Mount Stuart batholith showing host rock units, foliation pattern (largely magmatic in pluton), and location of studied stoped blocks. Gray line shows location of cross section through roof of batholith shown in Figs 3 and 4. D = location of dunite block (Fig. 5) and P = location of metapsammite block (Fig. 6). Bold lines show orientation of major structures in the batholith and host rock. Note that the foliation in the batholith smoothly cuts across internal contacts (shown with thin solid lines). Index shows location of this figure in Washington.

western end (Fig. 2). In the northeastern body of the Mount Stuart batholith, the mushroom-shaped region consists of tonalite and less common biotite–hornblende–quartz diorite that grades into biotite–hornblende granodiorite in its central part (Fig. 2). These rocks surround pyroxene–hornblende–quartz diorite and mafic tonalite in the northeastern part of the mushroom (Erikson, 1977; Anderson, 1992; Anderson

and Smith, 1995). Tonalite grades into granodiorite and locally two-mica granodiorite along the batholith margins in the sheet-like and hook-shaped regions (Anderson, 1992; Anderson and Smith, 1995).

This batholith intrudes two host rock units, the dominantly pelitic, multiply deformed Chiwaukum Schist and in the south the ophiolitic Ingalls Complex, which structurally overlies the schist (Miller, 1985; Tabor *et al.*, 1987) (Fig. 2). Contacts with the host rock are generally steep in the mushroom- and sheet-like regions and dip moderately to steeply away from the pluton at its northwestern end. Particularly in the mushroom-shaped and sheet-like regions of the batholith, topographic relief of ~2000 m provides some control on the vertical architecture of the batholith (Fig. 3). Small roof pendants and continuous sections of Chiwaukum Schist overlying the batholith in the central sheet-like region represent sections of the roof (Figs 3 & 4). Here, roof rocks preserve gently dipping foliations which are axial planar to isoclinal, typically recumbent folds. Although roughly parallel, the batholith–host rock contact is stepped in detail and discordant to host rock structures even at the scale of a few meters. Stoped blocks are commonly preserved up to a few hundred meters below the roof (Fig. 4) indicating that stoping occurred along the roof contact, at least during final emplacement of the magma. These stoped blocks preserve the same structures as seen in the roof rocks. Less common stoped blocks also occur > 1000 m below the roof contact (Fig. 3).

Aligned igneous minerals (plagioclase, orthopyroxene, hornblende, biotite) and mafic microgranitoid enclaves define a magmatic foliation and lineation. In the southeast zoned part of the batholith, the magmatic foliation generally has steep dips and defines a roughly margin-parallel pattern in map view (Fig. 2). Lineations are generally weak and have variable but typically steep plunges. About half way between the center and eastern margin of the southeast lobe, the magmatic foliation defines a margin-parallel zone where dip reversals define a fan-like pattern that changes laterally into a V-shaped synformal pattern (Fig. 2).

In the central sheet-like region, magmatic structures are well developed but vary in style and orientation both laterally and vertically (Figs 2–4). Steeply dipping foliation and subhorizontal lineation occur throughout much of the sill-like region. Flat-lying, roof-parallel foliation occurs between a few centimeters and tens of meters of roof contacts (e.g. Fig. 4b). At the northeast wall contact, magmatic foliation is margin-parallel and an intensely developed magmatic lineation ($L \gg S$ fabrics) plunges gently, whereas near the southwest margin a weak, steep lineation and steep, margin-parallel foliation ($S > L$ fabrics) is more common. Magmatic folds (i.e. hypersolidus folding of magmatic foliation, layering, or enclaves) with subhorizontal axes and steep NNE-dipping axial planes occur locally (Miller and Paterson, 1992, 1994).

In the northwest hook-shaped region, the magmatic foliation and lineation are only weakly to moderately developed. The foliation tends to strike NW and dip steeply, and the lineation trends NW–SE with variable plunges. However, in detail these structures show complicated patterns that include rapid variations in orientation. We interpret this pattern to reflect tens-of-meters to kilometer-scale magmatic folds, similar to those seen in the sheet-like region. Elsewhere we have speculated that the hook-shaped outline of this portion of the batholith may reflect one of these folds (Paterson *et al.*, 1994).

Beck *et al.* (1981) concluded from their paleomagnetic study of the Mount Stuart batholith that after emplacement the pluton was either tilted ~35° down to the southwest, translated northward > 2000 km, or some combination thereof. The uncertainty in their

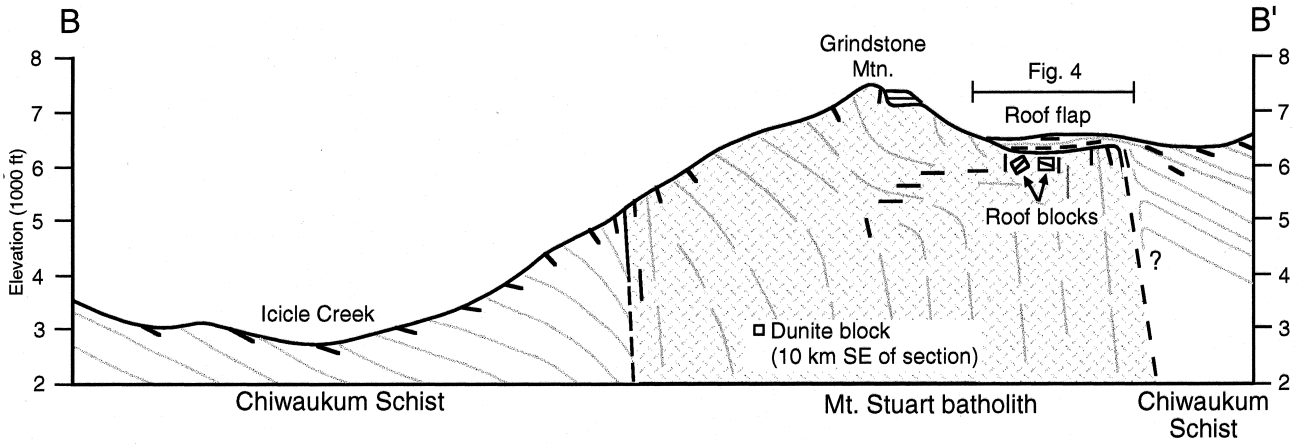

Fig. 3. Cross-section through the 'sheet-like' region of the Mount Stuart batholith (location shown in Fig. 2) showing location of stoped blocks below roof flaps and the approximate depth to the stoped blocks shown in Figs 5 and 6. Dark dashes = host rock and magmatic foliation measured at surface and/or projected into cross-section; light lines = inter-

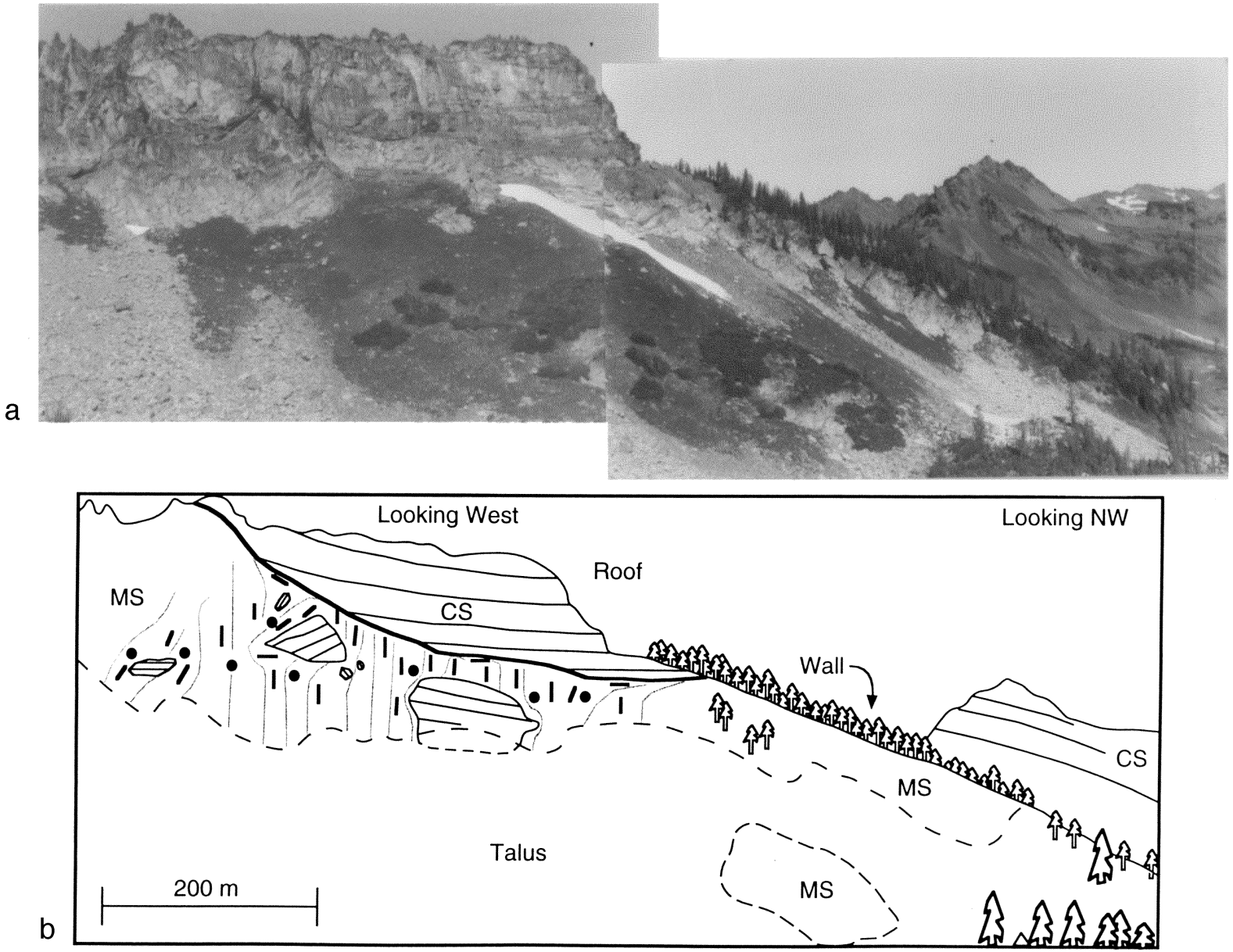

Fig. 4. Photograph (a) and line drawing (b) of roof flap (consisting of Chiwaukum Schist) and stoped blocks (metapelite, metapsammite, and amphibolite) immediately below the roof of the batholith. Section is approximately vertical. Dark dashes = measured magmatic foliation and black dots measured subhorizontal magmatic lineation trending approximately perpendicular to section; Light lines = interpretation of magmatic foliation patterns around the stoped blocks based on line drawings made in the field. This roof contact rolls over behind the tree-covered ridge into a wall contact dipping 75–85° away from the photo.

conclusions lay in the fact that they had no information about paleohorizontal during emplacement. Ague and Brandon (1996) determined a 'best-fit' paleohorizontal surface using Al-in-hornblende barometry and concluded that the batholith was only tilted a small amount and must therefore have been translated >2000 km. However, their conclusion remains controversial (see discussions in Anderson, 1997; Paterson and Miller, 1998; Brandon and Ague, 1998). In an attempt to determine paleohorizontal using settling of stoped blocks, we completed 1:6000 scale mapping and some hand drawings of stoped blocks of metapelite, metapsammite, and amphibolite in tonalite directly below the roof (Fig. 4). Here, using stoped blocks to determine paleo-plumb lines failed completely. No record of block settling is recorded by the foliation and lineation patterns. Instead, a generally steep magmatic foliation remains undeflected until a few meters or less from the blocks and in some places is not significantly deflected. Where deflections do occur they do not form patterns consistent with block settling, but instead indicate that the foliation was bent symmetrically around pre-existing blocks (Fig. 4b). This same magmatic foliation maintains its steep dips near the roof contact, commonly maintaining these orientations to within one meter of the contact. A strong subhorizontal, magmatic mineral lineation in this region also remains undeflected on all sides of the blocks. The surprisingly narrow to locally non-existent regions of deflections around these blocks have implications for viscosity contrasts and magma behavior, and are further discussed below.

These negative results in terms of determining paleohorizontal, but intriguing results in terms of timing of fabric formation, encouraged us to examine foliation patterns around stoped blocks in other parts of the batholith. In two cases we were able to find stoped blocks >1000 m below the roof in which two approximately perpendicular surfaces passed through the block. This allowed us to complete 1:1 scale tracings of magmatic foliaton patterns around these blocks on the two perpendicular planes in order to better depict foliation patterns in three dimensions (Figs 5 & 6). One of the blocks is a layered and metamorphosed

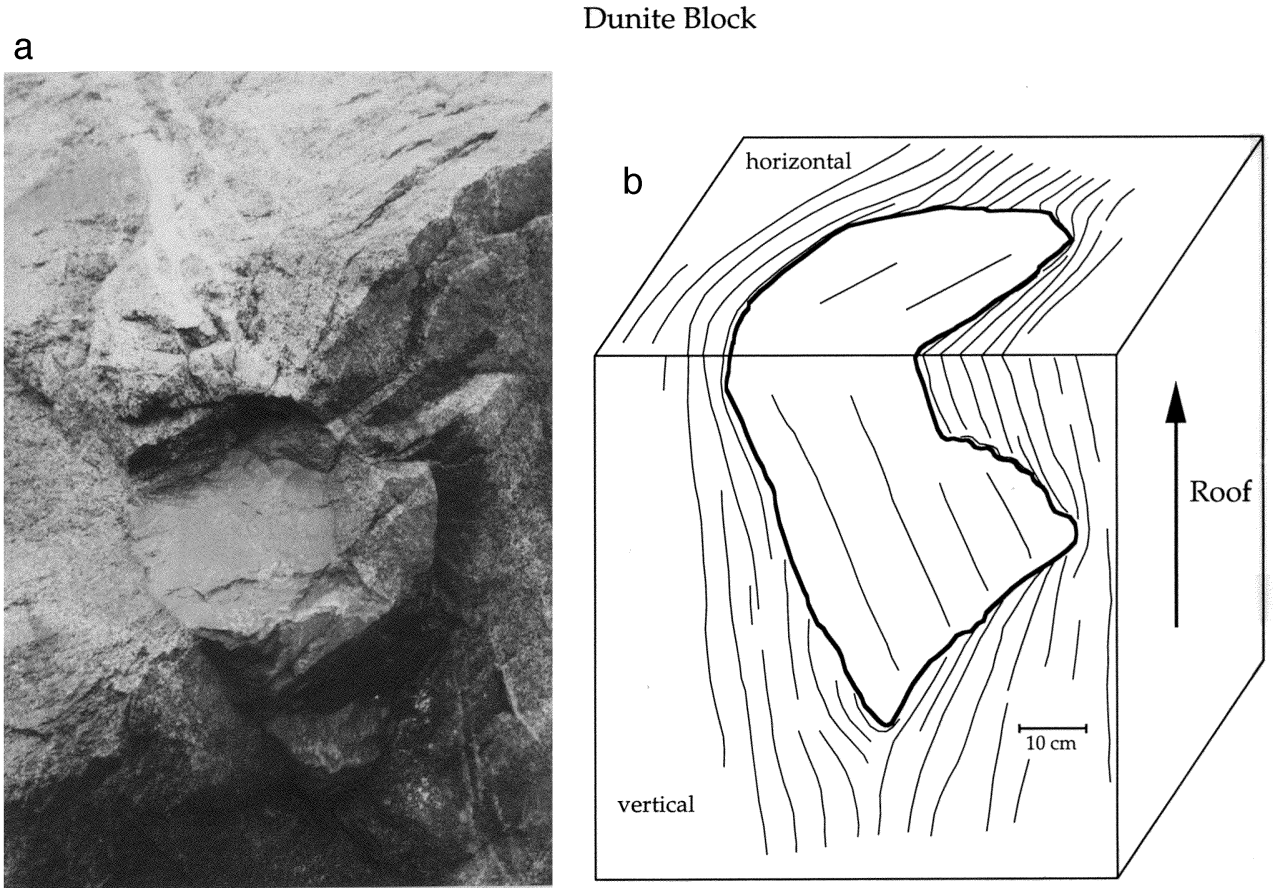

Fig. 5. Photograph (a) and block diagram (b) of magmatic foliation patterns around a dunite block (location shown as D in Fig. 2) measured on subhorizontal and subvertical joint surfaces. Diagram was constructed from 1:1 scale mylar tracings. Metamorphic layering in block shown with thin lines. Foliation trends in quartz diorite around block maintain the same orientations for tens to hundreds of meters away from block. Note alignment of block elongation parallel to regional foliation trend, lack of strong deflection at top end of block, foliation triple point at bottom corner, and inward facing and truncated arcuate pattern of foliation on left side of block.

dunite enclosed in quartz diorite (Fig. 5). The other block is a quartz-rich schist or immature metapsammite enclosed in diorite (Fig. 6). The latter block was probably derived from the Chiwaukum Schist, whereas the former was probably derived from the ophiolitic Ingalls Complex. Both blocks lie well within the mush-

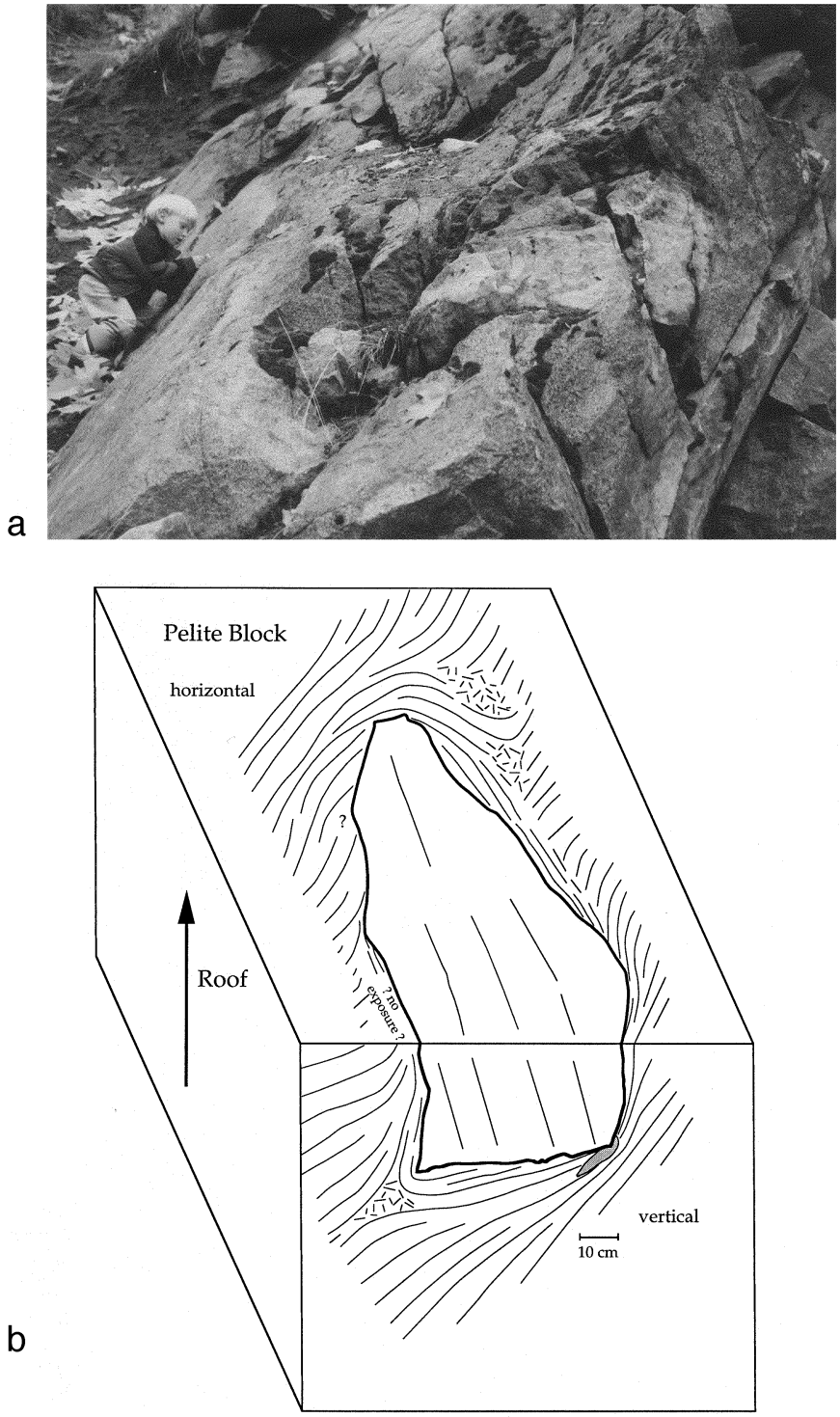

Fig. 6. Photograph (a) and block diagram (b) of magmatic foliation patterns around a metapsammite block with local metapelite layers (location shown as P in Fig. 2) measured on subhorizontal and subvertical joint surfaces. Diagram was constructed from 1:1 scale mylar tracings. Metamorphic layering in block shown with thin lines. Foliation trends in diorite around block maintain consistent orientations for tens of meters away from block. Note alignment of block long axis perpendicular to regional foliation trend, sharp transition from regional trends to block margin-parallel trends at the top and bottom of block on subhorizontal surface, foliation triple point at bottom corner of vertical face, inward facing and truncated arcuate pattern of foliation on several margins of block, and indented microgranitoid enclave at the upper right corner of the block on the vertical face.

room-shaped region (Figs 2 & 3), have sharp corners, form irregularly shaped 'rectangles', and preserve pre-emplacement host rock structures. There is little field evidence for melting of these blocks or contamination of the host magmas. However, we have not conducted geochemical studies to evaluate these interpretations.

Deflection patterns of magmatic foliation are again inconsistent with those expected from block settling and instead are compatible with bending of foliation around a preexisting object. For example, the long dimension of the dunite block (subparallel to internal layering) is aligned parallel to batholith-scale foliation trends (Fig. 5) and the long axis of the metapsammite block is perpendicular or parallel to foliation (Fig. 6), depending on how much of the upper part of the block has been removed by erosion, but neither have vertical long axes, the orientation predicted by settling in a viscous fluid (e.g. Tritton, 1988; Kerr and Lister, 1991). Furthermore, foliation deflection patterns are reasonably symmetric around the blocks rather than displaying flattening fabrics below and constrictional to chaotic fabrics above the blocks. Instead, cleavage triple points occur at the 'ends' of the blocks where batholith-scale foliation trends first approach the blocks. In these triple junctions, foliation is poorly defined in the plane of exposure. Finally, the batholith-scale foliation patterns are not deflected until short distances (<0.5 block radii) from each block and fabric intensities and sometimes deflections are not particularly strong near the blocks.

In detail, the magmatic foliation patterns near the blocks are quite complex. Around both blocks, the foliation locally defines inward curving arcuate patterns which are discordant to the block margin. At the top of the dunite block, foliation locally shows little deflection even at the block margin. Along one margin of the dunite block, foliation is roughly parallel to the margin, but here appears to be crenulated. The foliation pattern around the metapsammite block shows a strong discontinuity surface on two sides of the block where foliation with moderate deflections from regional trends abruptly switches to orientations parallel to the block margin. This transition occurs only a few centimeters from the block, that is about two to three times the average size of plagioclase or hornblende crystals defining the foliation.

At one corner of the metapsammite block, a microgranitoid enclave is aligned parallel to the magmatic foliation and is in contact with the block (Fig. 6). Here, the sharp metapsammite corner projects into the enclave several centimeters indicating that: (1) the enclave was still soft enough to deform, (2) shortening has caused the more rigid metapsammite block to pierce the less rigid enclave, and (3) the magmatic foliation is perpendicular to the maximum shortening direction. The latter conclusion is also supported by the relatively symmetrical pattern of deflection of the foliation around the stoped blocks (Figs 4–6).

DISCUSSION

The most obvious conclusion supported by these data is that the magmatic fabrics in this batholith preserve no record of the sinking or rotation of stoped blocks as they settled to their present positions. This provides further support for the conclusion of Fowler and Paterson (1997) that magmatic fabrics are poor recorders of total strain: strain formed during magma ascent, early emplacement, and during settling and rotation of the stoped blocks has been completely overprinted by strain of magma during and after the blocks were trapped at their present location. Because these fabrics record no information about the settling paths of the stoped blocks, the blocks in the Mount Stuart batholith cannot be used as paleo-plumb bobs.

The discordant roof contact and occurrence of relatively large stoped blocks immediately below the roof imply that stoping occurred during final ascent/growth of this chamber. We also argue below that the size, density (at least for the dunite), and rectangular shape (at least for the metapsammite) also indicate that the stoped blocks have not had a long residence time in the magma chamber. Because formation of magmatic fabrics post-dates trapping of the blocks, the fabrics must have formed during or largely after final chamber construction. This conclusion is supported by the observations that the magmatic fabrics cut across internal petrological contacts and that the orientations of the fabrics and magmatic folds in the sheet- and hook-like regions match those in the nearby host rock; the latter observations indicate that at least the fabrics in this part of the batholith formed during syn-emplacement regional deformation of the batholith (Miller and Paterson, 1994).

The timing of the fabrics relative to final chamber construction is more problematic, however, for the margin-parallel pattern in the mushroom-shaped part of the batholith. Such fabric patterns are sometimes thought to form during chamber expansion (Holder, 1979; Bateman, 1985) or convection (Schmeling *et al.*, 1988). But in this part of the Mount Stuart batholith, magmatic foliation also cuts internal petrological contacts, locally forms synformal or fan-like patterns, post-dates settling of stoped blocks, and, at least near the stoped blocks examined, was formed during relatively coaxial shortening perpendicular to the foliation. However, the smaller size of these blocks and lack of correlation with a nearby roof contact makes their residence time in the chamber, and thus timing of fabric formation, less certain.

In an effort to better constrain likely residence times, particularly of the latter stoped blocks, we used two-dimensional finite difference thermal models to evaluate the thermal–mechanical behavior of metapsammite and dunite blocks in diorite magma (Fig. 7). The effects of latent heat of magma crystallization and melting of stoped blocks, the possibility of both flow-

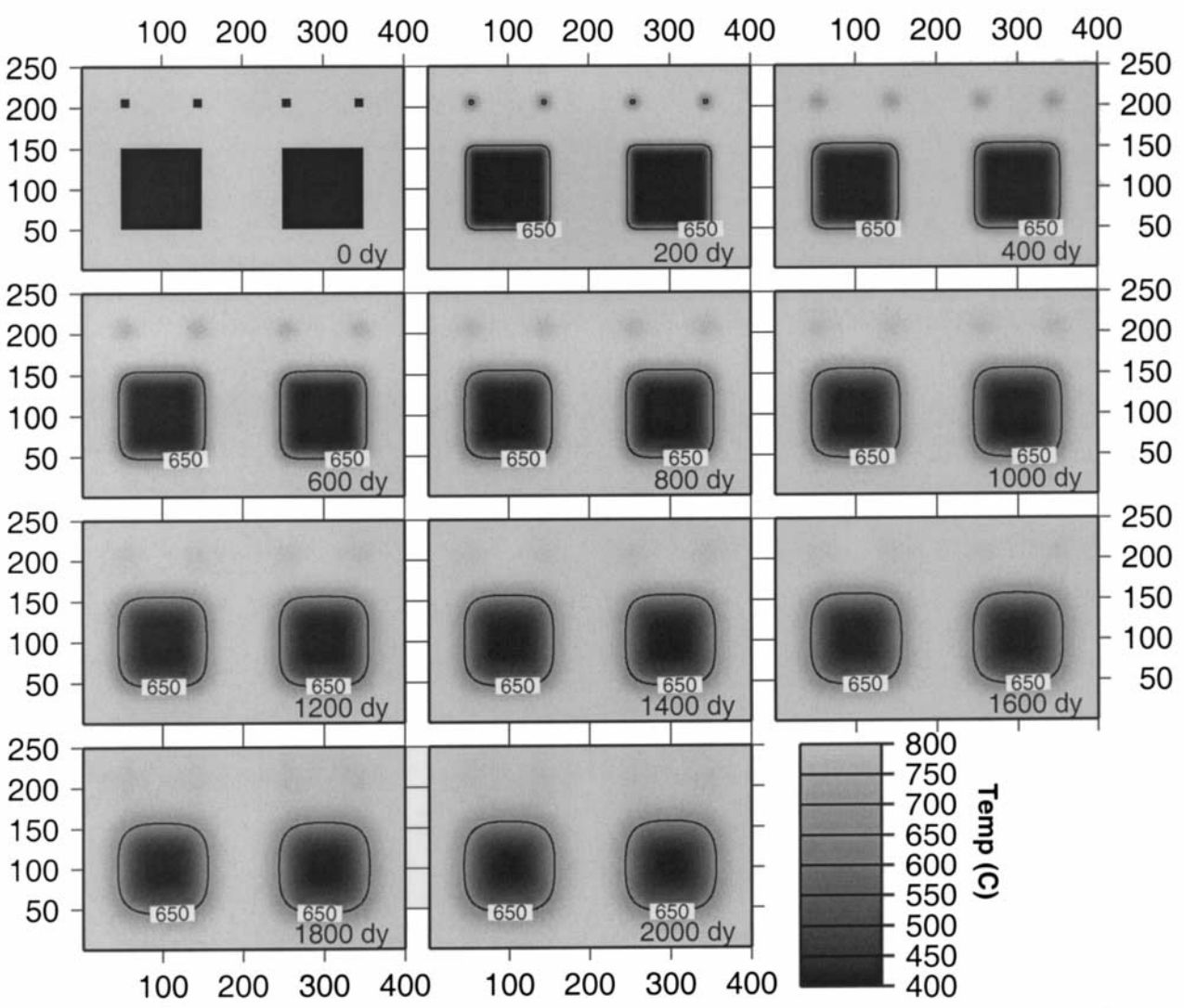

Fig. 7. Thermal conductive heating model for 10 m^2 and 100 m^2 dunite (left blocks in each box) and metapsammite blocks (right blocks in each box) with initial 400°C temperature in magma with starting temperature of 800°C. First box at time zero, each subsequent box = 200 day intervals (total 2000 days). 650°C isotherm shown for larger blocks. Note how small metapsammite blocks reach temperatures in excess of 750°C in several hundred days (i.e. they thermally disappear in the figure) as do the sharp corners of all the larger blocks.

ing and non-flowing magma near blocks, and the effect of block anisotropy on heat conduction are included in the modeling. Initial block shapes are assumed to be rectangles and to range in diameter from 10 to 100 m^2, that is significantly larger than the preserved blocks. For the dunite, initial temperature for the surrounding quartz diorite was set at 800°C, that is slightly higher than the crystallization temperature calculated from mineral equilibria at this location by J. L. Anderson (reported in Paterson *et al.*, 1994, Stop 2-2). For the metapsammite, initial magma temperature for the surrounding diorite was also set at 800°C, that is at the low end of temperatures calculated by Anderson at this locality (reported in Paterson *et al.*, 1994; Stop 1-6). Initial block temperatures were set at 400°C, probably somewhat below actual temperatures during stoping of these blocks as host rocks were at least at lower amphibolite facies during emplacement (Paterson *et al.*, 1994).

In all modeling runs with static melts, the 10 m^2 dunite blocks reached the magma temperature in about 2000 days (Fig. 7). Clarke *et al.* (1998) indicate that large blocks and/or initially cold blocks may undergo thermal cracking and thus rapid reduction in block size. Otherwise the dunite block is thermally stable because of its high melting temperature. The 10 m^2 metapsammite block (with local metapelitic layers) reached magma temperatures (> 750°C) in less than 600 days, and the thermally unstable corners of both large and small blocks reached such temperatures in as little as 200 days. Runs in which magma moves past the block, in which conduction increases parallel to anisotropy, and in which magma or block temperatures were higher decrease these times further. We thus

suggest that at least the metapelitic layers in the metapsammite block should have started to melt and disaggregate, particularly at its sharp corners within 200 days (Fig. 7). Thus, even if additional factors alter our heating rates by an order of magnitude, the sharp corners on the metapsammite block and lack of field evidence of melting suggest a short residence time in the magma (see also Marsh, 1982; Furlong and Myers, 1985). Likely rapid settling rates of these blocks also imply that either the density of the magma matches that of the blocks (not a reasonable assumption for the dunite) or that viscosity and/or yield strength of the magma was high enough to stop block sinking. In either case, these conclusions again imply that the blocks have not resided for long times in the chamber, since the dunite did not sink out of sight and the metapsammite did not melt. They also suggest that the magma was near its solidus when the fabrics formed because of the lack of evidence for block melting and need for moderately high viscosities and thus high crystal contents (see below). Thus, in this batholith the stoped blocks are good chronometers, probably representing the last blocks to form during chamber growth. Therefore the bending of fabrics around the blocks support formation of these magmatic fabrics largely after magma emplacement.

The symmetrical pattern of foliation deflections around blocks both near and far from the roof argue for largely coaxial flattening during fabric formation. This intriguing conclusion is supported by the presence of symmetrical magmatic folds and constrictional, typically orthorhombic fabrics near the roof blocks (Miller and Paterson, 1994). We have not verified, however, whether such orthorhombic fabrics are widespread in this batholith.

Magma viscosity estimates

Because the magmatic foliations are deflected around the blocks, the viscosities of the magmas at the time of fabric formation must have been less than the least viscous block, that is around 10^{18}–10^{20} Pa s for the weaker metapsammite (Cristescu, 1989; Shea and Kronenberg, 1992; Kohlstedt *et al.*, 1995). However, viscosities must have been high enough to support the most dense block, assuming that the blocks were still negatively buoyant. The density of the metapsammite block is estimated at 2.80 g cm^{-3} (e.g. Daly *et al.*, 1966; Olhoeft and Johnson, 1989), whereas that of the dunite is estimated at 3.27 g cm^{-3} (e.g. Daly *et al.*, 1966; Olhoeft and Johnson, 1989). Densities of the diorite and quartz diorite magmas, calculated using procedures outlined in McBirney (1993), were 2.65–2.67 g cm^{-3} for temperatures between 850°C and 700°C at the dunite locality, and from 2.66 to 2.69 g cm^{-3} for the same temperature range at the metapsammite locality. Melt viscosites calculated for each locality fell between 10^4 and 10^6 Pa s using methods outlined in McBirney (1993) and assuming Newtonian, crystal poor melts (e.g. $<40\%$ crystals). These data indicate that both blocks were negatively buoyant and that the dunite block in particular should have sunk rapidly in a low viscosity, crystal-poor magma. For example, assuming 10^5 Pa s for the magma viscosity, the densities reported above, and an approximate radius of 1 m for the blocks, and utilizing Stokes settling for static, Newtonian melts, then settling rates of 2.72×10^{-3} and 3.3×10^{-2} m s^{-1} are predicted for the metapsammite and dunite, respectively. In order for the blocks to settle very slowly (e.g. <10 cm per 1000 years), or essentially to be frozen in to allow foliation to develop after settling, requires even higher viscosities. Magma viscosities of 10^{13} yield settling rates of 3.6 and 17.5 cm per 1000 years for the metapsammite and dunite, respectively. Essentially a viscosity of 10^{14}–10^{15} is needed in order to get the dunite to sink at less than 2 cm per 1000 years.

These viscosity estimates determine the 'effective' or 'apparent' viscosity of magma, that is the tangent line to the stress–strain rate curve, and thus ignores any effect of yield strength or power law behavior. Sparks *et al.* (1977) have argued that magmas may have yield strengths and thus lower the viscosity needed to support objects. Using solutions plotted in their fig. 1 and data for our dunite block (excess density of ~0.6, g cm^{-3} and diameter of 100 cm), we estimate that a yield strength of ~750–800 N m^{-2} is needed to support this block, that is twice the value of the highest yield strength measured by Sparks *et al.* (1977) in magma with ~50% crystals. We therefore argue that to get yield strengths high enough to support the blocks in the Mount Stuart batholith would again require crystal-rich magmas, particularly for the large blocks near the pluton roof. However, the existence of a yield strength would reduce by one to two orders of magnitude the melt viscosities needed to trap the blocks (see fig. 3 in Sparks *et al.*, 1977)

There remains uncertainty about whether evidence used in support of yield strengths in magmas may instead indicate power law behavior (e.g. see Webb and Dingwell, 1990; Dingwell *et al.,* 1993; and Fernandez and Gasquet, 1996 for full discussion). Unfortunately, several parameters needed to use power law equations are so poorly constrained in our examples that we have not attempted to calculate block sinking in a power law material. Nevertheless, power law behavior of magma near blocks should increase block settling rates and thus require higher viscosities to trap the blocks.

It would be nice to use the above viscosity or yield strength estimates to determine the crystal content of the magma and thus know how near the solidus fabrics formed (e.g. Nicolas and Ildefonse, 1996). Unfortunately the relationship between viscosity and crystal percent in magmas is complex and depends on composition (e.g. Ryan and Blevins, 1987), pressure

and temperature (e.g. Kushiro, 1980; Scaillet *et al*., 1997), volatile content (e.g. Scaillet *et al*., 1997), and strain rate (Webb and Dingwell, 1990). Emplacement pressure (300–400 MPa), temperature (~800–700°C), and compositions are well known for the Mount Stuart batholith (Paterson *et al*., 1994; Anderson and Smith, 1995). Although less well constrained in our study, we note that an increase in volatile content and strain rate will lower magma viscosities and therefore require even higher crystal percents or lower temperatures to get the high viscosities needed to support the stoped blocks. We also note that all plots of viscosity vs percent crystals presently published indicate that the viscosities needed in our example require high crystal percents (>70%) and temperatures at or near the diorite solidus (e.g. Wickham, 1987; Miller *et al*., 1988; Cruden, 1990; Lejeune and Richet, 1995; Scaillet *et al*., 1997). Thus we believe that the estimated viscosities, and/or need for large yield strengths, are compatible with our conclusion that the magma must have been crystal-rich (>70% crystals) and with our earlier conclusion that the diorite magma must have been near its solidus during fabric formation. This result is compatible with conclusions of Berger *et al*. (1996) who estimated a viscosity of $\sim 10^{16}$ Pa s during emplacement of the Bergell pluton (Swiss and Italian Alps), by Nicolas and Ildefonse (1996) who estimated a viscosity of from $\sim 10^{14}$ to 10^{16} Pa s during formation of magmatic fabrics in crystal-rich (>80%) gabbro from the Oman ophiolite, and by Scaillet *et al*. (1997) who argued that in felsic granitoids (with H_2O contents of from 4 to 7 wt%) the greatest increase in crystal content and viscosity occurs just above solidus temperatures. The latter authors thus determined that "mineral fabrics preserved in granites probably do not reflect the intrusion mechanism", a conclusion supported by our data.

Given the above conclusions it is intriguing to further consider the implications of the fabric patterns near the blocks. We suggest that the lack of foliation deflection near some block margins, the inward facing arc patterns, and the local abrupt discontinuities in fabric patterns, imply that these features formed in relatively static magmas in which the alignment of igneous crystals reflects the complex strain field around more resistant objects. We imagine that large reorientations of pre-existing fabrics would have first occurred around the rigid blocks as they settled. Then subsequent shortening would begin to reorient individual crystals perpendicular to the regional shortening axis by a combination of filter pressing, contact melting, and melt-aided grain boundary sliding (e.g. Park and Means, 1996; Nicolas and Ildefonse, 1996). Immediately adjacent to the blocks, the XY principal plane of strain was refracted parallel to the block margins causing crystals in strain shadows or along block margins not to realign perpendicular to the regional shortening direction. The discontinuities near the metapsammite block reflect this transition between crystals that reoriented themselves during regional shortening vs those too near the block to do so. It is probable that magma near the stoped blocks crystallized slightly before magma farther away, thus helping to preserve the margin parallel fabrics.

CONCLUSIONS

Magmatic fabric patterns around stoped blocks potentially provide a range of useful information such as paleohorizontal during pluton emplacement and the timing, kinematics, and magma viscosities during fabric formation. In the Mount Stuart batholith, the stoped blocks fail to record information about paleohorizontal, but do indicate that the magmatic fabrics formed largely after chamber construction, during coaxial strain, and when magma viscosities were relatively high (from 10^{14} to 10^{15} Pa s) and/or magmas had developed significant yield strengths. Clearly, more sophisticated analyses of kinematics and viscosity values than those presented above are possible. It is our hope that by presenting these examples from the Mount Stuart batholith others will be encouraged to look for and examine similar features in other plutons and attempt more sophisticated analyses.

Acknowledgements—This research was supported by NSF Grants EAR-8916325 and EAR-8917343 awarded to Paterson and Miller, respectively. We thank J. Lawford Anderson for discussions about geochemical data from the Mount Stuart batholith, David Okaya and Aaron Yoshinobu for help with the thermal modeling, Chris Hill for help with drafting figures, and Sandy Cruden and Jean Luc Bouchez for reviews of the manuscript. Paterson also wishes to thank Benoit Ildefonse for his hospitality and discussions while finishing this manuscript at Montpellier.

REFERENCES

Ague, J. J. and Brandon, M. T. (1996) Regional tilt of the Mount Stuart batholith, Washington, determined using aluminum-in-hornblende barometry: Implications for the northward translation of Baja British Columbia. *Geological Society of America Bulletin* **108,** 471–488.

Anderson, J. L. (1992) Compositional variation within the high-Mg, tonalitic Mount Stuart batholith, north Cascades, Washington. *Geological Society of America Abstracts with Programs* **24,** 3.

Anderson, J. L. (1997) Regional tilt of the Mount Stuart batholith, Washington, determined using aluminum-in-hornblende barometry: Implications for northward translation of Baja British Columbia: Comment. *Geological Society of America Bulletin* **109,** 1223–1225.

Anderson, J. L. and Smith, D. R. (1995) The effects of temperature and oxygen fugacity on the Al-in-hornblende barometer. *American Mineralogist* **80,** 549–559.

Bateman, R. (1985) Aureole deformation by flattening around a diapir during *in-situ* ballooning: the Cannibal Creek granite. *Journal of Geology* **93,** 293–310.

Beck, M. E., Jr, Burnmester, R. F. and Schoonover, R. (1981) Paleomagnetism and tectonics of the Cretaceous Mount Stuart Batholith of Washington: translation or tilt? *Earth and Planetary Science Letters* **56,** 336–342.

Bergantz, G. W. and Dawes, R. (1994) Aspects of magma generation and ascent in the continental lithosphere. In *Magmatic Systems*, ed. M. P. Ryan, pp. 291–317. Academic Press, San Diego, California.

Berger, A., Rosenberg, C. and Schmidt, S. M. (1996) Ascent, emplacement and exhumation of the Bergell pluton within the southern steep belt of the central Alps. *Schweizerische Mineralogische und Petrogrephische Mitt*. **76,** 357–382.

Brandon, M. T. and Ague, J. J. (1998) Regional tilt of the Mount Stuart batholith, Washington, determined using aluminum-in-hornblende barometry: Implications for northward translation of Baja British Columbia: Reply. *Geological Society of America Bulletin* **110,** 687–690.

Buddington, A. F. (1959) Granite emplacement with special reference to North America. *Geological Society of America Bulletin* **70,** 671–747.

Clarke, D. B., Henry, A. S. and White, M. A. (1998) Exploding xenoliths and the absence of 'elephant graveyards' in granite batholiths. *Journal of Structural Geology* **20,** 1325–1343.

Cristescu, N. (1989) *Rock rheology*. Kluwer Academic, Dordrecht.

Cruden, A. R. (1988) Deformation around a rising diapir modeled by creeping flow past a sphere. *Tectonics* **7,** 1091–1101.

Cruden, A. R. (1990) Flow and fabric development during diapiric rise of magma. *Journal of Geology* **98,** 681–698.

Daly, R. A., Manger, G. E. and Clark, S. P. (1966) Density of rocks. In *Handbook of Physical Constants*, ed. S. P. Clark. Geological Society of America Memoir **97**.

Dingwell, D. B., Bagdassarov, N. S., Bussod, G. Y. and Webb, S. L. (1993) Magma rheology. In *Short Course Handbook on Experiments at High Pressure and Applications to the Earth's Mantle*, ed. R. W. Luth, pp. 131–196. Mineralogical Association Canada, **21**.

Erikson, E. H. (1977) Petrology and petrogenesis of the Mount Stuart batholith–Plutonic equivalent of the high-alumina basalt association? *Contributions to Mineralalogy and Petrology* **60,** 183–207.

Fernandez, A. G. and Gasquet, D. R. (1996) Relative rheological evolution of chemically contrasting coeval magmas; example of the Tichka plutonic complex (Morocco). *Contributions to Mineralogy and Petrology* **116,** 316–326.

Fowler, T. K., Jr and Paterson, S. R. (1997) Timing and nature of magmatic fabrics in plutons from relations around arrested stoped blocks. *Journal of Structural Geology* **19,** 209–224.

Furlong, K. P. and Meyers, J. D. (1985) Thermal–mechanical modeling of the role of thermal stresses in magma contamination. *Journal of Volcanology and Geothermal Research* **24,** 179–191.

Gay, N. C. (1968) Pure shear and simple shear deformation of inhomogeneous viscous fluids. 2. The determination of the total finite strain in rocks from objects such as deformed pebbles. *Tectonophysics* **5,** 295–302.

Haeussler, P. J. and Paterson, S. R. (1993) Post-emplacement tilting and burial of the Guadalupe Igneous Complex, Sierra Nevada, California. *Geological Society of America Bulletin* **105,** 1310–1320.

Holder, M. T. (1979) An emplacement mechanism for post-tectonic granites and its implications for their geochemical features. In *Origin of Granite Batholiths: Geochemical Evidence*, eds M. P. Atherton and J. Tarney, pp. 116–128.

Kerr, R. C. and Lister, J. R. (1991) The effects of shape on crystal settling and on the rheology of magmas. *Journal of Geology* **99,** 457–467.

Kohlstedt, D. L., Evans, B. and Mackwell, S. J. (1995) *Strength of the lithosphere: constraints imposed by laboratory experiments Journal of Geophysical Research* **100,** 17,587–17,602.

Kushiro, I. (1980) Viscosity, density, and structure of silicate melts at high pressures and their petrological applications. In *Physics of Magmatic Processes*, ed. R. B. Hargraves, pp. 93–120. Princeton University Press, Princeton.

Lejeune, A-M. and Richet, P. (1995) Rheology of crystal-bearing silicate melts; an experimental study at high viscosities. *Journal of Geophysical Research* **100,** 4215–4229.

Marsh, B. D. (1982) On the mechanics of igneous diapirism, stoping, and zone melting. *American Journal of Science* **282,** 808–855.

McBirney, A. R. (1993) *Igneous Petrology*. Jones and Bartlett Publishers, Boston.

Miller, C. F., Watson, E. B. and Harrison, T. M. (1988) Perspectives on the source, segregation and transport of granitoid magmas. *Transactions Royal Society of Edinburgh: Earth Sciences* **79,** 135–156.

Miller, R. B. (1985) The ophiolitic Ingalls Complex, north-central Cascades Mountains, Washington. *Geological Society of America Bulletin*. **96,** 27–42.

Miller, R. B. and Paterson, S. R. (1992) Tectonic implications of syn- and post-emplacement deformation of the Mount Stuart batholith for mid-Cretaceous orogenesis in the North Cascades. *Canadian Journal of Earth Sciences* **29,** 479–485.

Miller, R. B. and Paterson, S. R. (1994) The transition from magmatic to high-temperature solid-state deformation: implications from the Mount Stuart batholith, Washington. *Journal of Structural Geology* **16,** 853–865.

Nicolas, A. (1992) Kinematics in magmatic rocks with special reference to gabbros. *Journal of Petrology* **33,** 891–915.

Nicolas, A. and Ildefonse, B. (1996) Flow mechanism and viscosity in basaltic magma chambers. *Geophysical Research Letters* **23,** 2013–2016.

Olhoeft, G. R. and Johnson, G. R. (1989) Densities of rocks and minerals. In *Practical Handbook of Physical Properties of Rocks and Minerals*, ed. R. S. Carmichael, pp. 139–176. CRC Press, Boca Raton, Florida.

Park, Y. and Means, W. D. (1996) Direct observation of deformation processes in crystal mushes. *Journal of Structural Geology* **18,** 847–858.

Paterson, S. R. and Miller, R. B. (1988) Regional tilt of the Mount Stuart batholith, Washington, determined using aluminum-in-hornblende barometry: Implications for northward translation of Baja British Columbia: Comment. *Geological Society of America Bulletin*. **110,** 685–687.

Paterson, S. R., Fowler, T. K., Jr and Miller, R. B. (1996) Pluton emplacement in arcs: a crustal-scale exchange process. *Transactions of the Geological Society Edinburgh, Earth Sciences* **87,** 115–123.

Paterson, S. R., Miller, R. B., Anderson, J. L., Lund, S., Bendixen, J., Taylor, N. and Fink, T. (1994) Emplacement and evolution of Mount Stuart batholith. In *Geologic Field Trips in the Pacific Northwest, Geological Society of America Annual Meeting*, eds D. A. Swanson and R. A. Haugerud, pp. 2F–1–2F-47.

Ryan, M. P. and Blevins, J. Y. K. (1987) *The Viscosity of Synthetic and Natural Silicate Melts and Glasses at High Temperatures and One Bar (10^5 Pascals) Pressure and at Higher Pressures*. United States Geological Survey Bulletin, **1764**.

Scaillet, B., Holtz, F. and Pichavant, M. (1997) Rheological properties of granitic magmas in their crystallization range. In *Granite: From Segregation of Melt to Emplacement Fabrics*, eds J. L. Bouchez, D. H. W. Hutton and W. E. Stephens, pp. 11–29. Kluwer Academic, Dordrecht.

Schmeling, H., Cruden, A. R. and Marquart, G. (1988) Finite deformation in and around a fluid sphere moving through a viscous medium: implications for diapiric ascent. *Tectonophysics* **149,** 17–34.

Shea, W. T. and Kronenberg, A. K. (1992) Rheology and deformation mechanisms of an isotropic mica schist. *Journal of Geophysical Research* **97,** 15,201–15,237.

Sparks, R. J. S., Pinkerton, H. and Macdonald, R. (1977) The transport of xenoliths in magmas. *Earth and Planetary Science Letters* **35,** 234–238.

Tabor, R. W., Frizzell, V. A., Whetten, J. T., Waitt, R. B., Swanson, D. A., Byerly, G. R., Booth, D. B., Hetherington, M. J. and Zartman, R. E. (1987) *Geologic Map of the Chelan 30-minute by 60-minute Quadrangle*. U. S. Geological Survey Map I—1661. USGS, Washington.

Tritton, D. J. (1988) *Physical Fluid Dynamics*. Oxford Science Publications, Clarendon Press.

Webb, S. L. and Dingwell, D. B. (1990) Non-Newtonian rheology of igneous melts at high stresses and strain rates: experimental results for rhyolite, andesite, basalt, and nephelinite. *Journal of Geophysical Research* **95,** 15,695–15,701.

Wickham, S. M. (1987) The segregation and emplacement of granitic magmas. *Journal Geological Society London* **144,** 281–297.